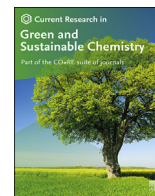




Contents lists available at ScienceDirect

Current Research in Green and Sustainable Chemistry

journal homepage: www.elsevier.com/journals/current-research-in-green-and-sustainable-chemistry/2666-0865



Emerging technologies for treatment of antibiotic residues from wastewater influent/effluent for sustainable environment: A case study with NFC-doped titania immobilized on polystyrene as an efficient technology



Reyhan Ata^a, Gunay Yildiz Tore^{b,*}, Maulin P. Shah^c

^a Çerçezköy Vocational School of Namık Kemal University, Tekirdağ 59860, Turkey

^b Environmental Engineering Department of Çorlu Engineering Faculty, Namık Kemal University, 59860, Tekirdağ, Turkey

^c Industrial Waste Water Research Lab, Division of Applied & Environmental Microbiology, Enviro Technology Limited, Ankleshwar, India

ARTICLE INFO

Keywords:

NFC-Doped TiO₂
Polystyrene
Antibiotic residues
Urban and industrial wastewater
Sustainable environment
Emerging technology

ABSTRACT

In this study, 5 urban and 2 industrial wastewater treatment plants (WWTPs) were investigated. Raw wastewaters and effluents of WWTPs were characterized in terms of both organic and inorganic pollutants and antibiotic residues. According to the analysis results; organic pollutants for raw wastewaters and influents in urban WWTP were measured between 412 and 921 mg L⁻¹ for COD, 345–421 mg L⁻¹ for TOC, 61–160 mg L⁻¹ for COD, 48–83 mg L⁻¹ for TOC, respectively. However, in industrial WWTPs, these values were determined in raw wastewaters between 1404 and 2367 mg L⁻¹ for COD, 821–826 mg L⁻¹ for TOC and in effluents between 272 and 408 mg L⁻¹ for COD and 97–208 mg L⁻¹ for TOC, respectively.

In addition, in the characterization study of antibiotic residues by the results of HPLC/MS-MS measurements, the amounts of Ciprofloxacin (from the fluoroquinolones), Erythromycin (from the macrolides group) and Sulfamethoxazol (from the sulfonamide group), which are one of the three main groups of antibiotics in the waste water samples, were found in high amounts in both urban and industrial WWTPs despite the biological treatment process. More antibiotic residues (Erythromycin-ERY, Ciprofloxacin-CIP and Sulfamethoxazol-SMX) were detected in untreated raw wastewater compared to effluent wastewater. While CIP antibiotic was not found only one urban WWTP, the highest amounts in the effluents of 4 urban WWTPs were measured between 13,800 ng L⁻¹ and 38,800 ng L⁻¹. Moreover, ERY is only detected in high amount in one urban WWTP raw and effluent wastewater as 23,100 ng L⁻¹ and 5430 ng L⁻¹, respectively. The SMX was detected in 2 separates urban WWTPs at a value of 19,700 ng L⁻¹ in the raw wastewater sample and at a value 10,100 ng L⁻¹ in effluent sample of another urban WWTP. Antibiotic residue removal ratios after Advanced Oxidation Process using specially prepared NFC-doped TiO₂ photocatalyst immobilized on polystyrene (PS) cup inner surface at amount 0.45 g were determined as 97%–100% for CIP, 100% for ERY, 86%–100% for SMX, 57%–64% for COD and 61,5%–72% for TOC, respectively.

According to the above mentioned results, this study proved that photocatalytic oxidation processes performed under visible light with a specially prepared immobilized form (PS/Cup-NFC-0.45 g) photocatalyst provide higher antibiotic removal from both urban and industrial wastewater. Thus, these results showed us that if the application of NFC-doped Titania, immobilized on polystyrene, can be integrated with an appropriate reactor design on the real/pilot scale, this technology can be proposed as an efficient technology for sustainable environment.

1. Introduction

Recent researches have revealed that antibiotics have detrimental effects on the reproductive system of all living life, and besides these harmful effects they create alone, they cause more and more damages

with a synergistic effect when combined [1]. Antibiotics, which are defined as persistent pollutants that have been polluting the environment and directly affecting the habitat, although they are in relatively low concentrations in secondary treatment wastewater, can also cause the formation of pathogens that will resist some bacteria [2–4].

* Corresponding author.

E-mail address: gyildiztore@nku.edu.tr (G.Y. Tore).

<https://doi.org/10.1016/j.crgsc.2021.100065>

Received 4 November 2020; Received in revised form 1 February 2021; Accepted 2 February 2021

Available online 26 March 2021

2666-0865/© 2021 Elsevier Ltd. All rights reserved.

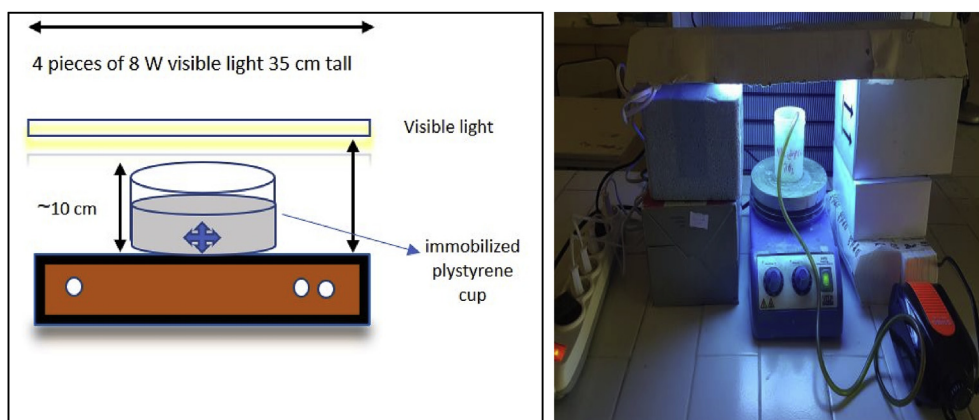


Fig. 1. Schematic representation and photo of photocatalytic oxidation test by using immobilized PS/Cup-NFC photocatalyst.

Table 1
LOD, LOQ and Recovery results.

	LOD (ng/L)		
	CIP	ERY	SMX
	150	60	200
	LOQ (ng/L)		
	CIP	ERY	SMX
	450	180	600
Recovery %	100	71	62
Accuracy (%)	99,5	99,3	95,6

In a study, conducted by Le-Minh et al., in 2012, has been scientifically demonstrated that even very low antibiotic concentrations in treated wastewater can cause toxic effects on various types of water and resistance in natural bacterial populations [5]. In the same year, Gao et al. found that only 25–30% of antibiotics are metabolized after use by humans or animals, and 60–75% do not change as their own active ingredients or are excreted from the body as metabolites and released in to wastewater [6].

In general, most of the antibiotics that have been tested to date have not been easily removed from waste water under aerobic conditions. The persistence of antibiotics and releasing in to the environment in increasing rates, cause the formation of antibiotic-resistant bacteria, which has led to an increase in research on the detection and removal of antibiotic residues in the areas where the wastewater is discharged. In recent years, very valuable studies have been carried out showing that secondary treatment as a conventional method are insufficient to prevent these systems to threat the most of the antibiotics that are being used

Table 2
Real urban and industrial wastewaters' conventional and antibiotic characterization.

Sampling Point	pH		COD mg.L ⁻¹		TOC mg.L ⁻¹	CIP ng.L ⁻¹	ERY ng.L ⁻¹	SMX ng.L ⁻¹
	Interval	Average	Interval	Average	Average			
WWTP-1 Urban Influent	7,7-7,7	7,3	241-554 ^a	412	~389 ^b	7190	263	6130
WWTP-1 Urban Effluent	7,4-8	7,6	51-111 ^a	85	83 ^b	26400	<0	5310
WWTP-2 Urban Influent	7,2-8	7,6	322-588 ^a	486	421 ^b	24900	<0	19700
WWTP-2 Urban Effluent	7,5-8	7,7	60-67 ^a	62	48 ^b	16,100	2950	5140
WWTP-3 Urban Influent	7,3-7,6	7,4	271-550 ^a	457	408 ^b	7280	4100	5350
WWTP-3 Urban Effluent	7,7-5	7,3	56-70 ^a	61	52 ^b	13800	4680	10100
WWTP-4 Urban Influent	7,5-8	7,7	107-310 ^a	209	–	–	–	–
WWTP-4 Urban Effluent	7,6-8	7,8	57-70 ^a	64	48 ^b	16100	2950	5140
WWTP-5 Urban Influent	8,4	8,4	921	921	345	9170	23100	5610
WWTP-5 Urban Effluent	8,3	8,3	160	160	60	14000	5430	4970
WWTP-6 Org.Ind. Dist.Influent	7,6-9,6	8,9	904-2151 ^a	1404	821 ^b	<0	<0	19700
WWTP-6 Org.Ind. Dist.Effluent	8-8,7	8,2	229-307 ^a	272	208 ^b	<0	<0	5100
WWTP-7 Leather Org.Ind. Dist. Influent	6,4-7,5	7,1	1881-3092 ^a	2367	826 ^b	<0	<0	2890
WWTP-7 Leather Org.Ind. Dist.Effluent	7,9-8,2	8	198-805 ^a	408	97 ^b	<0	<0	2990

^a June–November (Measured seasonal values in June and November).

^b Average of June and November.

more and more day by day [2–4,6–9]. In addition, other scientific studies have shown that antibiotic-resistant genes frequently occur in wastewater, groundwater, drinking water, sludge, soil and sediment [2–4,6,10, 11].

In a study conducted by Zhang et al. (2009), it was stated that low amounts of antibiotics discharged into the environment without being completely treated, could cause much more harmful and complex effects when combined than their effects own alone, on living organisms [1–3]. The results of all these studies revealed the necessity of a comprehensive assessment of the possible environmental impacts of antibiotics due to the serious and irreversible increase in discharges to the receiving environment. Yalap and Balcioglu (2008) [12] and Rickman and Mezyk (2010) [7] emphasized the urgency of developing alternative treatment methods in the control of antibiotics, which are called new generation pollutants and discharged to the receiving environment through industrial, domestic or hospital waste water treatment facilities [7,12]. In this context, especially in areas where agricultural activities are carried out, it is inconvenient to use antibiotic residues in treated water without removing them, and advanced oxidation processes have gained importance in removing antibiotics [1,12,13].

Titania is one of the most used photocatalysts in developing AOPs in recent years due to its low cost, low solubility and toxicity, and high chemical stability [14,15]. As a research subject, titania-based heterogeneous photocatalysts, used in pre-treatment and post-treatment AOP applications of Conventional Wastewater Treatment Plants (CWWTPs), have been among the interesting subjects that have been investigated in recent years in the removal of many refractory pollutants such as antibiotics in water and wastewater [16]. Another important feature of

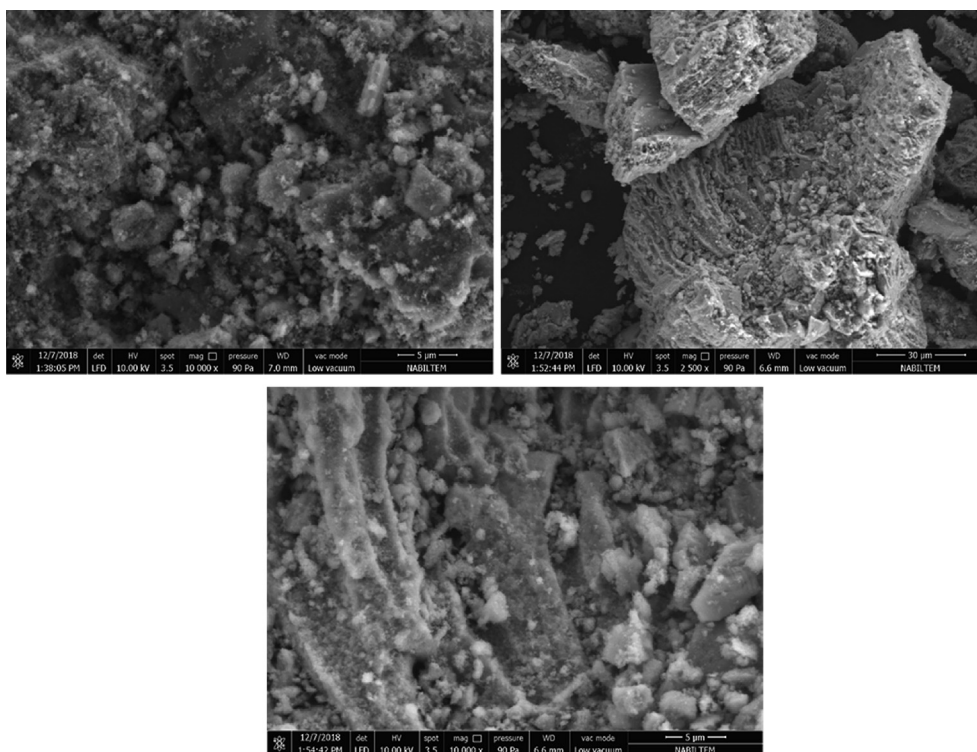
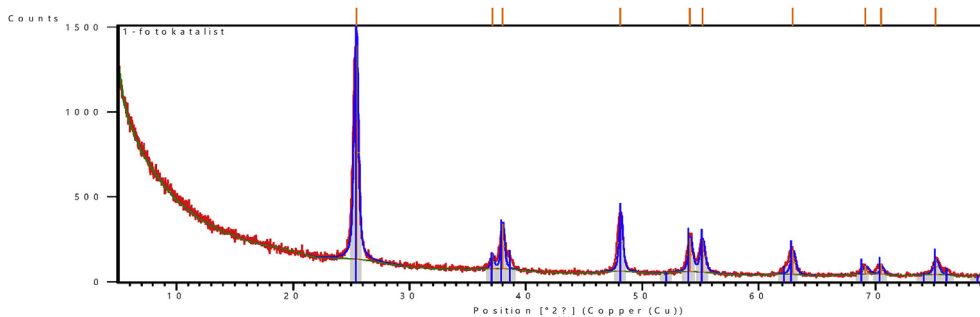


Fig. 2. SEM Results - The morphology of powdered NFC-doped TiO_2 photocatalyst, specially prepared in laboratory.



Graph 4. XRD analysis results of powdered NFC- TiO_2 .

Table 3

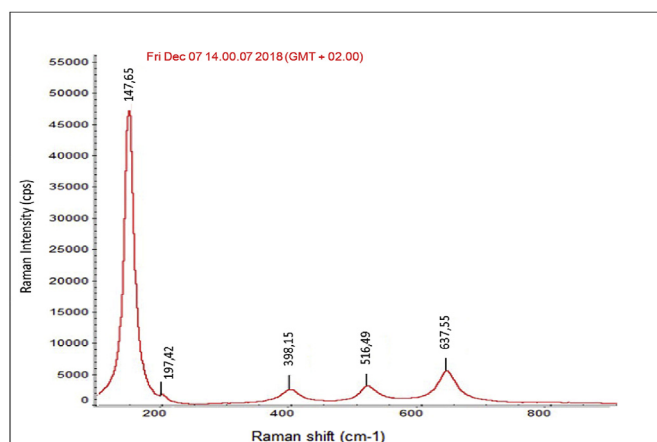
Wavelengths of Raman Scattering events for TiO_2 .

	E_g	E_g	B_{1g}	A_{1g}	E_g
TiO_2	143	196	396	514	637

tania is its ability to absorb approximately 4% of solar radiation from the earth's surface. Thus, when this energy is equal to or higher than the space energy in the band of the semiconductor catalyst, it induces the formation of the hydroxyl radical with the highest electron absorption, and a large number of low-degradability contaminants can be easily oxidized by this radical [17–19].

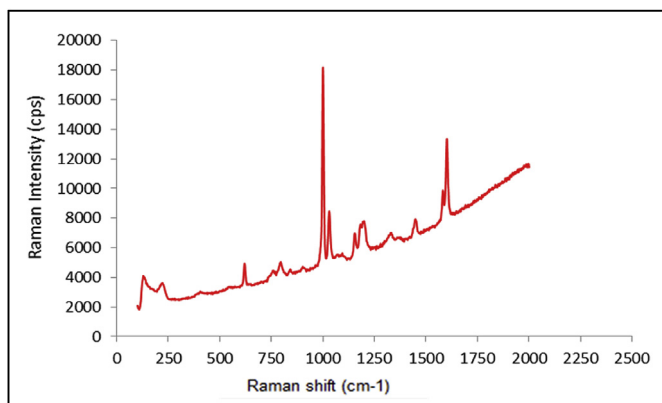
In the literature, many studies have been reported that Titania is doped with different elements (Nitrogen, Carbon, Fluoride, Phosphorus, Sulfur, etc.) as single, double or triple under visible light irradiation to increase photoabsorption capability [20–25].

In recent studies in the literature, there are studies using immobilized photocatalysts prepared using Titania and different materials in different reactor configurations. Miranda-García et al., in their studies conducted in 2010 and 2014 [26], showed that the Titania mixture (sol gel TiO_2 and

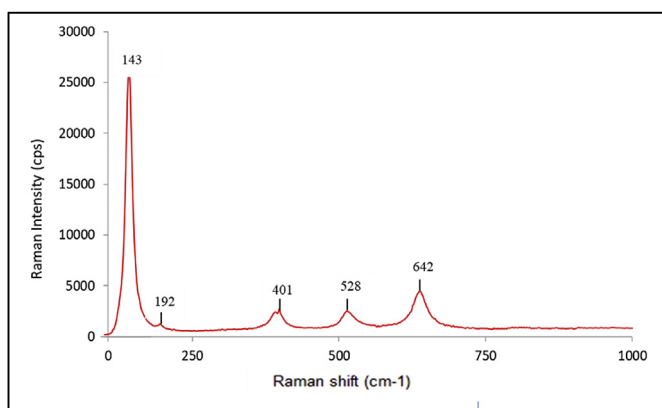


Graph 5. Raman shift results of NFC-doped TiO_2 .

TiO_2 -P25), coated on glass spheres by immobilization method, is an effective method for removing pesticides in wastewater using different



Graph 6. Raman shifts of empty cup (Uncoated cup).



Graph 7. Raman shifts of Immobilized PS/Cup-NFC-Doped TiO₂.

types of reactors. In addition, in many studies in the recent literature, it has been reported that pharmaceutical residues and dyes in wastewater can be removed successfully by using TiO₂-P25 fixed on the glass ball surface by UVC radiation.

It is a worrying fact that medicines, antibiotics and personal care

products, which are defined as the next generation activators with organic content, cannot be completely removed by biological processes (different mechanisms such as biodegradation, evaporation, air stripping and adsorption on primary or secondary sludge) in order to ensure the sustainability and continuity of agriculture. In addition, the presence of organic pollutants and primary degradation products in the influent wastewater can inhibit biological processes in wastewater treatment plants. Since conventional wastewater treatment plants cannot adequately remove antibiotics that are not biodegradable, the presence of antibiotic residues in the receiving waters where the wastewater is discharged restricts the sustainable use of surface waters, especially used for agricultural irrigation. In order to eliminate this restriction, the scientific world has focused on effective, cheap and easily applicable advanced oxidation processes in recent years.

Considering all these studies, one of the important points is to remove refractory pollutants in wastewater, as well as to develop a cheaper and easily applicable method and type of reactor. For this purpose, we developed triple-doped Titania nanomaterial (powdered NFC-doped added TiO₂) as a continuation of our previous work and in this work, which is an even more advanced stage, and achieved in removing antibiotic residues from domestic and industrial wastewater [16,27-31]. We have demonstrated through experimental studies that it can be reused for irrigation [16]. So the aim of this study, as a continuation and further step of this work, carried out in 2019, specially prepared powdered NFC-doped TiO₂ photocatalyst was immobilized in a laboratory-scale photocatalytic reactor obtained by plastering it on polystyrene (PS) polymer which is a cheap, inert and non-toxic thermoplastic polymer with low density. Antibiotic residues were treated and evaluated from raw wastewater and five urban and two industrial wastewater treatment plant effluents.

2. Material VE method

2.1. Characterization of raw and effluent wastewaters

5 urban (Malkara-WWTP-1, Lüleburgaz- WWTP- 2, Kırklareli- WWTP- 3, Enez- WWTP- 4, Karpuzlu- WWTP- 5) and 2 industrial (Çerkezköy Organized District WWTP-6, Çorlu Leather Organized District WWTP-7) CWWTPs were investigated in this study. Raw and effluent samples were taken from inlet and outlet of all WWTPs at summer, autumn and spring months according to the TS ISO 5667-10 standart. Hach HQ40D

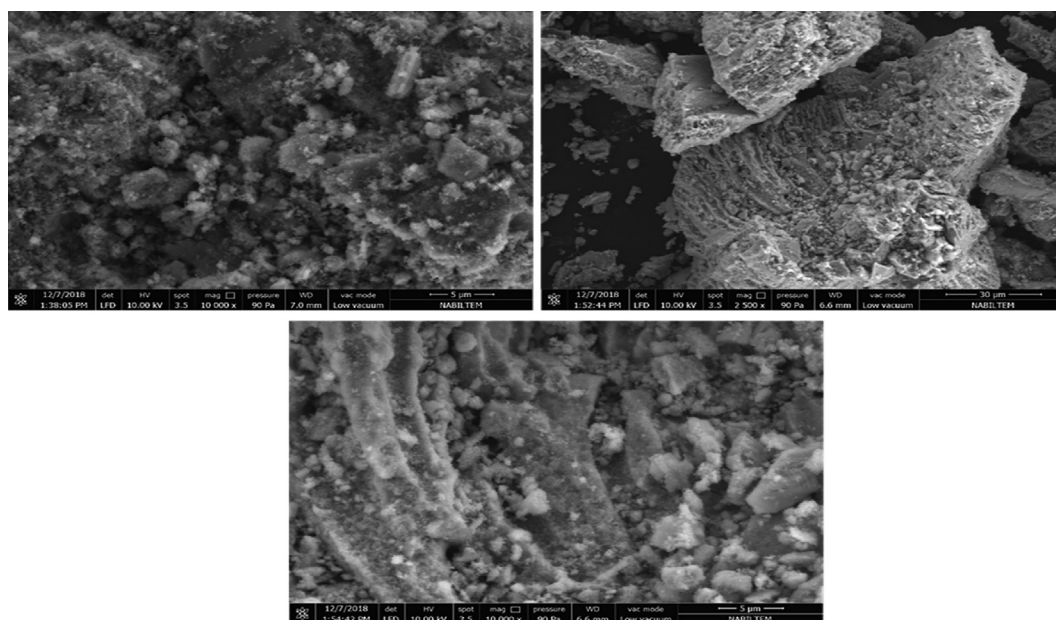


Fig. 3. The morphology of Immobilized PS/Cup-NFC-Doped TiO₂ (SEM Results).

Table 4
The HPLC/MS-MS results.

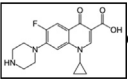
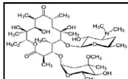
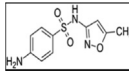
	Antibiotic concentration (Before AOP)			Antibiotic concentration in immobilized PS/Cup-NFC/0,45 g photocatalyst (After AOP)		
	CIP ng/L	ERY ng/L	SMX ng/L	 CIP (ng/L)	 ERY (ng/L)	 SMX (ng/L)
WWTP-1 Urban Effluent	38800	263	6120	<0	213	<0
WWTP-2 Urban Effluent	16100	2950	5140	<0	191	700,36
WWTP-3 Urban Effluent	13800	4680	10100	<0	362	<0
WWTP-5 Urban Effluent	14000	5430	4970	<0	<0	605,8
WWTP-6 Org.Ind.Distr. Effluent	<0	<0	5100	<0	<0	686,16

Table 5
Antibiotic removal efficiencies.

	Removal Eff. % CIP	Removal Eff. % ERY	Removal Eff. %SMX
WWTP-1 Urban Effluent	~100	99,45	~100
WWTP-2 Urban Effluent	~100	98,81	86,37
WWTP-3 Urban Effluent	~100	97,38	~100
WWTP-5 Urban Effluent	~100	~100	87,81
WWTP-6 Org.Ind.Distr. Effluent	~100	~100	86,55

Multimeter was used for the parameters measured simultaneously with sampling. All analysis were done according to the APHA 1998 except COD and Color. COD and Color analysis were carried out according to the international standards [32–34].

Çerkezköy (with approximately 267 factory) and Çorlu Organized Industrial Zones (with approximately 100 factory), including pharmaceutical, chemical, leather and such processing plants, are two of Turkey's largest and most established industrial zones. There are 17 pharmaceutical factories only in Çerkezköy Organized Industrial Zone. Settlement plant of the zone is given in supplementary file.

2.2. Powder form photocatalyst preparation

The NFC-doped TiO₂ sample was prepared and characterized [35]. The re-prepared NFC-doped TiO₂ photocatalyst in powder form according to the sol-gel method, was precipitated and the precipitate was washed with distilled water. After centrifugation, after calcination process for 2 h at 450 °C NFC-doped TiO₂ was characterized.

2.3. Immobilization of photocatalyst by using PS

In order to immobilize of NFC-doped TiO₂ photocatalyst by means of by coating the inner wall of the PS material (PS/Cup) preferred as the polymeric substrate (available from Microglass Heim, Internal Diameter = 8.5 cm, weight = 7.187 g). In this immobilization study, two different volumes of PS/Cups (70 mL and 200 mL) were used.

A 70 mL PS/Cup was used in the photocatalytic oxidation study for decolorization, and since more samples were needed for HPLC/MS-MS measurements, a 200 mL PS/Cup was used in the oxidation study for antibiotic removal. The excess NFC–TiO₂ particles on the inner surface of the PS containers were removed by processing several cycles in the ultrasonic bath (Bandelin Sonorex) until a stable load obtained on NFC–TiO₂/PS Cup. The NFC–TiO₂/PS containers were then left to dry for 48 h at room temperature and were named as NFC–TiO₂/PS- α , where α PS explained the amount of powdered NFC–TiO₂ (in grams) immobilized on the PS material surface. PS/Cups were plastered with NFC-doped TiO₂ powder form photocatalysts, which have been previously prepared in 0.3 and 0.45 g each, to ensure maximum contact with the wastewater. The immobilized photocatalysts in this PS/Cups form were named as PS/Cup-NFC/0.3 g and PS/Cup-NFC/0.45 g respectively. These PS/Cups were used in photocatalytic oxidation studies for photocatalytic activity, photocatalytic oxidation removal of antibiotic residues and

decolorization of real urban and industrial wastewater samples. The PS cup which not coated by NFC–TiO₂ powder was named as “Empty Cup”.

2.4. Testing stabilization capability of immobilized photocatalysts

In order to determine the stability of PS/Cup-NFC photocatalysts, the test was repeated 4 times successively in a row to measure that the antibiotic removal efficiency of the photocatalyst did not change during photocatalytic oxidation in urban or industrial wastewater.

2.5. Prepared photocatalyst particles' and PS-Cups' characterization

Photocatalysts were characterized by Dispersive Raman Spectroscopy (Thermo, DXR Raman) combined with 532–785 nm laser in spatial resolution 1 μ m and depth resolution 2 μ m in the 150–1000 cm⁻¹ range in the central laboratory of NKU-NABILTEM. Scanning Electron Microscope (SEM) analysis was performed using the FEI-QUANTA FEG 250 equipped with Everhardt Thornley ETD, STEM and EDS detectors, which can reveal micro and nano-sized structures of materials.

2.6. Determination of photocatalytic activity test

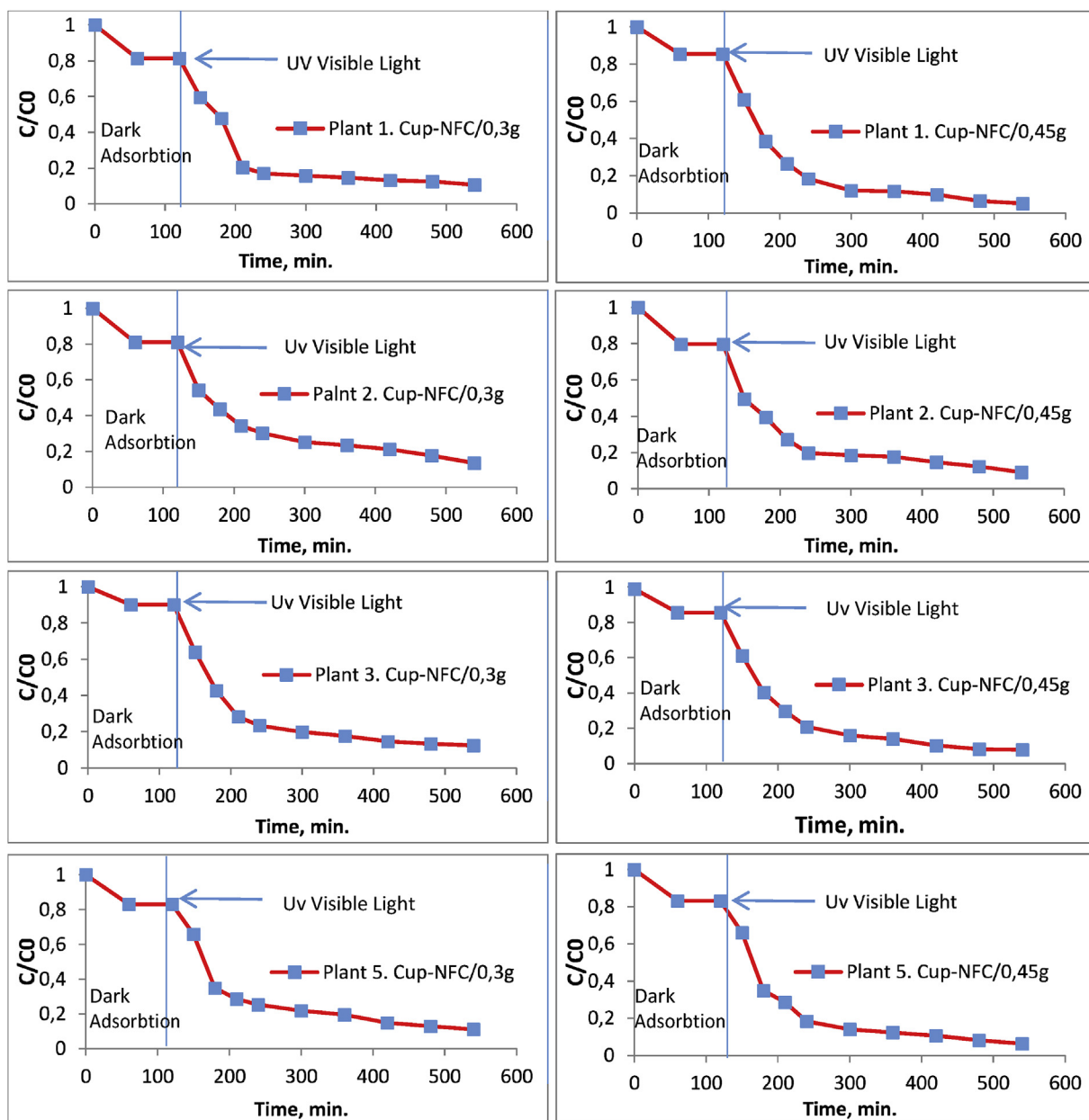
Photocatalytic oxidation studies, for the removal of antibiotic residues and decolorization of urban and industrial effluents, carried out in the PS/Cup-NFC photoreactor, were shown in Fig. 1.

200 mL PS Cups which was obtained by immobilizing the specially prepared NFC-doped TiO₂ photocatalyst was used as photoreactors equipped with mini air pump (Qair = 150 cm³ min⁻¹) and a magnetic stirrer (Jeiotech Multi Channel Stirrer). Experiments were carried out by using 120 mL real urban and industrial wastewaters, separately. Irradiation was provided by 4 cylindrical UV visible light lamps with a length of 35 cm and 8 W nominal power for each, lamp at 450–700 nm wavelength emission. Sample collecting (10–15 mL) were performed at a constant intervals during the photocatalytic tests. Test reactor was operated in the dark for 1 h and then 420 min (7 h) under visible light until to reach the adsorption equilibrium. Treated samples taken hourly through the reactor at determined time intervals were centrifuged for 15 min at 4000 rpm for sediment removal prior to analysis.

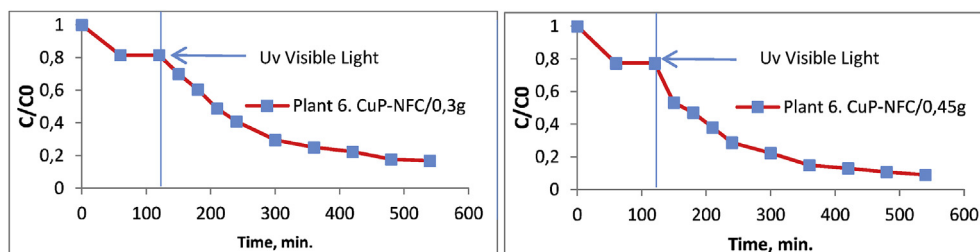
In order to monitor the reduction of TOC and antibiotic residues in wastewater samples, both absorbance (at λ = 663 nm in the UV-Vis spectrophotometer, determined by testing at different wavelengths) and total organic carbon (TOC) measurements (catalytic combustion at T = 680 °C with TOC were done on upper phase of the centrifuged samples.).

2.7. Method validation for antibiotic determination

In order to determine the antibiotic content of the raw wastewaters and effluents of the examined WWTPs, all samples were filtered by 0,45 μ filter before the extraction (SPE) carried out under pH 4 to 6 interval by filtering Oasis HLB cartridges. Each sample was then individually injected into HPLC/MS-MS with acetonitrile and methanol mobile phase C8 column (100 mm, 3 \times 2.7 μ m). According to this method, recovery efficiencies for ERY, CIP and SMX were calculated as 70%, 100% and 62%,



Graph 8. UV-Vis Spectrophotometer measurement results for PS/Cup-NFC/0,30 g and PS/Cup-NFC/0,45 g for urban samples.



Graph 9. UV-Vis Spectrophotometer measurement results for PS/Cup-NFC/0,30 g and PS/Cup-NFC/0,45 g industrial sample according to the UV-Vis results.

respectively. Thus, the results were considered as high validation that all three antibiotics could be accurately measured with the specified HPLC column.

3. Results and discussion

3.1. Method validation results

In this study, Solid Phase Extraction (SPE) and Recovery Method,

Table 6

Antibiotic removal efficiencies with immobilized PS/Cup-NFC/0,45 g photocatalyst after AOP according to the UV-Vis results.

	Removal Eff. % PS/Cup-NFC/0,3 g	Removal Eff. % PS/Cup-NFC/0,45 g
WWTP-1 Urban Effluent	90	95
WWTP-2 Urban Effluent	87	91
WWTP-3 Urban Effluent	89	94
WWTP-5 Urban Effluent	87	92
WWTP-6 Org.Ind.Distr. Effluent	83	87

which is explained in detail in “Material & Method” section, is used for extraction and recovering antibiotic residues from the raw influent (input) wastewater of urban and industrial WWTPs and studied samples provided from the effluent (output) wastewater of biological treatment process. The analytical limits, detection limits (LOD) and quantity limits (LOQ) were determined by validating the European Directive/657/EC in line with the criteria of accuracy, sensitivity, recovery and selectivity. In line with the data received in positive ESI + mode, LOD, LOQ and recovery results are given in Table 1.

Calibration peaks of standard stock solutions of ERY, CIP and SMX antibiotics at two different pH (pH 2 and pH 5) are also given at Graph 3.1 and Graph 3.2 together, with HPLC/MS-MS (Tandem-Sequential Quadropole Mass Spectrometry).

As seen in Graph 3.1 and Graph 3.2, it was preferred to study at pH 5, where the single and most prominent peak for the ERY antibiotic, the same intensity peak for the SMX antibiotic and the more intense peak for the CIP antibiotic were determined. The calibration kinetics of standard ERY, CIP and SMX antibiotic solutions verifying all these SPE analysis conditions are also presented in Graph 3.3.

Table 7

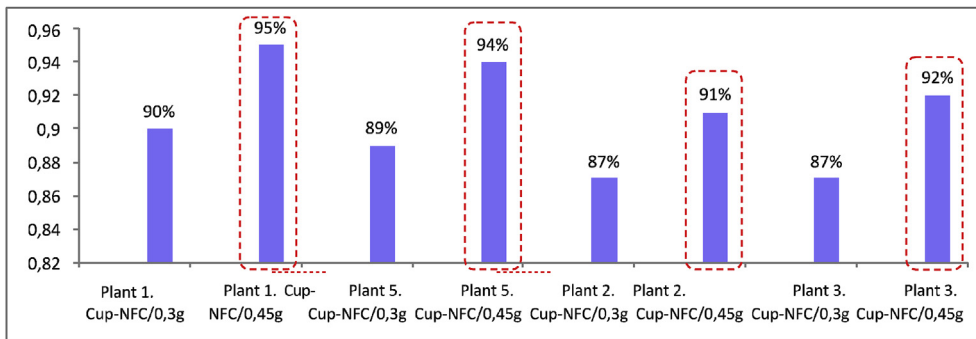
COD and TOC removal from biologically treated effluents from urban and industrial effluents with PS Cup-NFC/0.45 g photocatalysts immobilized by NFC-doped TiO₂.

	Before AOP	After AOP	COD Removal Eff. (%)	Before AOP	After AOP	TOC Removal Eff. (%)
	COD (mg.L ⁻¹)			TOC (mg.L ⁻¹)		
WWTP-1 Urban Effluent	94	40	57	83	27	67
WWTP-2 Urban Effluent	67	24	64	48	15	69
WWTP-3 Urban Effluent	70	27	61	52	20	61,5
WWTP-5 Urban Effluent	160	63	61	60	22	63
WWTP-6 Org.Ind.Distr. Effluent	229	98	57	208	58	72

As shown in Graph 3.3, the kinetic correlation coefficient (R) of all three antibiotics was calculated as approximately 1. This proves that this SPE method is the correct method and validation to be applied for solid phase extraction and recovery of the studied antibiotics. The main product peaks and mass/charge (*m/z*) ratios of main product peaks and metabolites, obtained as a result of HPLC/MS-MS measurements for determining CIP, ERY and SMX antibiotic residues, also confirmed these results. As a result of all these studies, recovery rates of antibiotics were determined as 62% for SMX, 100% for CIP and 71% for ERY.

3.2. Wastewater characterization results

Characterization results of real urban and industrial wastewaters



Graph 10. Comparison of photocatalytic activities of immobilized PS/Cup-NFC/0.3 g and PS/Cup-NFC/0.45 g photocatalysts in investigated urban wastewater.

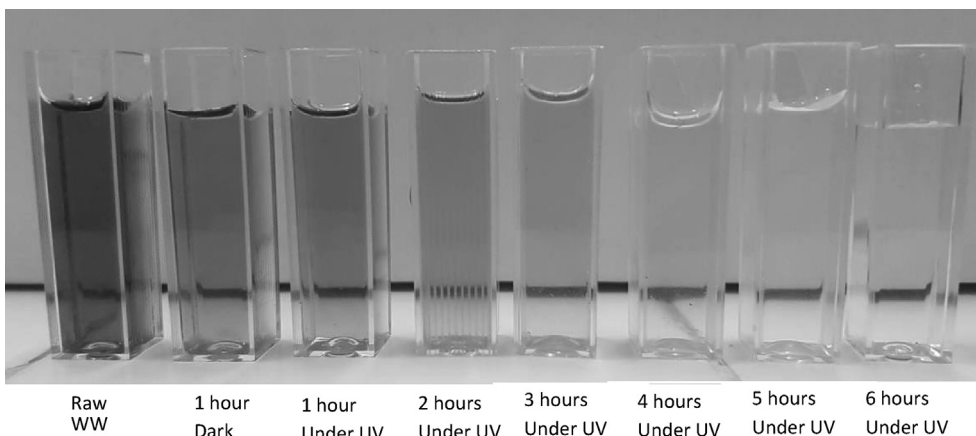


Fig. 4. Picture of color removal in WWTP-6. Org.Ind. Distr.Effluent with PS/Cup-NFC/0.45 g photocatalysts.

Table 8^aColor removal efficiency results of PS/Cup-NFC/0.45 g photocatalysts.

WW	Absorbance Interval	Before AOP Color, m ⁻¹	Water Quality Class	After AOP Color, m ⁻¹	Water Quality Class
WWTP- 1 Eff., Urban	436 525 620	1,8 0,8 0,6	First Class	0,0 0,0 0,0	First Class
WWTP- 5 Eff., Urban	436 525 620	3 1,5 0,8	Second Class	0,0 0,0 0,0	First Class
WWTP- 3 Eff., Urban	436 525 620	1,4 0,4 0,4	First Class	0,0 0,0 0,0	First Class
WWTP- 2 Eff., Urban	436 525 620	1,8 0,9 0,2	First Class	0,0 0,0 0,0	First Class
WWTP- 6 Org.Ind.Distr. Eff.	436 525 620	27,6 21,6 17,1	Fourth Class	2,21 0,28 0,11	First Class

^a August 10, 2016 and Official Gazette No. 29327, "Implementing Regulation on the Amendment of the TSWQR, Annex-5: Table 2. Quality Criteria by Classes in terms of General Chemical and Physicochemical Parameters of the International Surface Water Resources.

were given at Table 2 based on conventional (pH, COD, TOC) parameters and antibiotic (CIP, ERY, SMX) contents.

As illustrated in Table 2, according to the Turkish Surface Water Quality Regulation (TSWQR)-Annex 5 [36], low concentrations of organic pollutants were detected in the WWTP-1 in July. Moreover, while urban WWTP's samples of WWTP-2, WWTP-3 and WWTP-4 were characterized as low-polluted, they presented as medium-polluted character at Spring and Autumn months in terms of COD. Besides, influents of urban WWTPs (2, 3 and 4) had high-polluted characterization as TOC content. In addition, as expected, influents of WWTP-6 And WWTP-7 exhibited high contaminated organic contents in terms of COD values, while both industrial wastewater treatment plants have 4th class of water quality as bot influent and effluent water in July, according to TSWQR Annex 5 [36].

However, it is understood that both urban and industrial wastewater treatment plants met their discharge limits and managed to raise the wastewater quality to 1st and 2nd class in November and March.

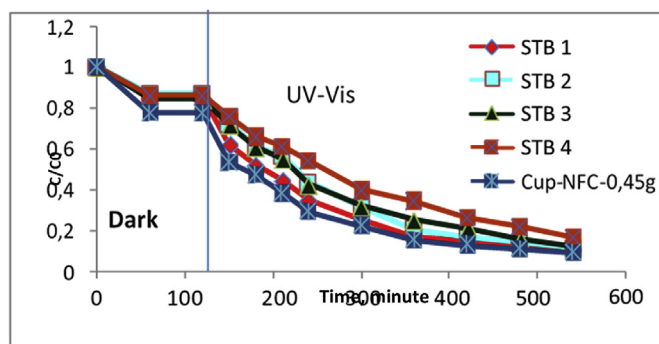
According to the validation study results, it was found that ERY, CIP and SMX antibiotics included in three main antibiotic groups (macrolides-, fluoroquinolones-, Sulfonamides-) were meaningful to measure at all WWTPs wastewater samples. Recovery yields were determined as 70% for ERY, 100% for CIP, 62% for SMX, respectively.

Contrary to expectations, the higher antibiotic contents were measured in effluent wastewater than influent wastewater of WWTPs. Most of antibiotics in feces can form complexes with soluble organic substances and their degradation may decrease and remain stable. Some

Table 9

Evaluation of treated effluents by photocatalytic oxidation with immobilized PS/Cup-NFC/0,45 g photocatalyst.

Waste Water	Before AOP				After AOP				
	DO (mg.L ⁻¹)	Water Quality Class*	Conductivity (mS.cm ⁻¹)	Water Quality Class*	DO (mg.L ⁻¹)	Water Quality Class*	Conductivity (mS.cm ⁻¹)	Water Quality Class*	Salinity (mg.L ⁻¹)
WWTP-1 Eff.,Urban	8,5	First Class	0,5	Class-1	10,7	First Class	0,37	First Class	237
WWTP-2 Eff.,Urban	6,5	Second Class	0,4	Class-1	8,5	First Class	0,34	First Class	218
WWTP-3 Eff.,Urban	5,8	Second Class	0,4	Class-1	7,5	First Class	0,35	First Class	224
WWTP-5 Eff.,Urban	7,0	Second Class	0,9	Class-2	9,5	First Class	0,68	First Class	435
WWTP-6 Org.Ind. Distr. Eff.	6,6	Second Class	2,7	Class-3	6,5	Second Class	1,85	Second Class	1184

**Graph 11.** Stabilization test results of immobilized PS/Cup-NFC/0.45 g photocatalyst.

antibiotics may be henced in feces during biological treatment [37,38]. Then after biological treatment, these antibiotics or their metabolites may be either released or recycled to the main compounds in waste water. The degree of degradation and mobility of an antibiotic between solid and aqueous phases may depend on the properties of the antibiotic (chemical bond structure) and hydrological effects. More research is needed to understand the biodegradation kinetics of antibiotics and the potency and mobility of degraded products of various antibiotics in different environments.

Antibiotic measurement results of effluent wastewater samples revealed that he highest amount of CIP antibiotic was measured in WWTP-1, WWTP-2, WWTP-4, WWTP-5 urban effluent water. WWTP-5 urban effluent water has the highest amount of ERY. SMX was detected in the highest amount of antibiotic in the effluent water of WWTP-2 urban effluent.

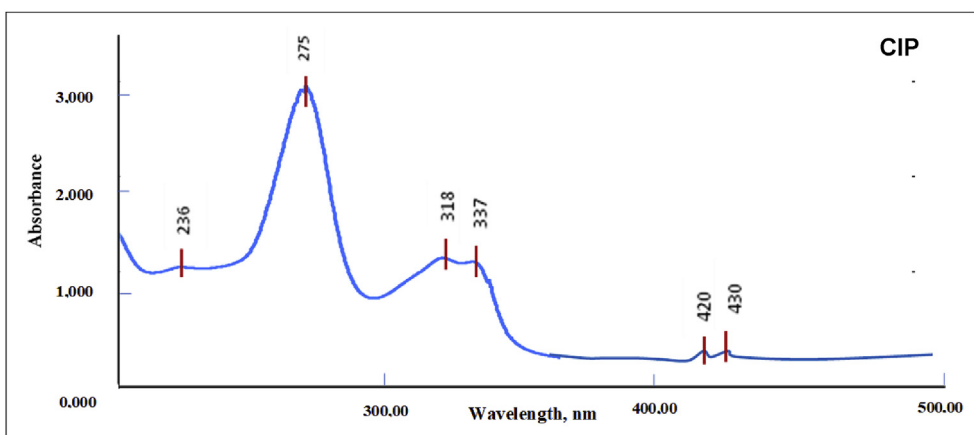
The influent wastewater measurements results showed that SMX was the highest amount of antibiotic in WWTP-6 and WWTP-7 Approximately 6.6 times higher amount of SMX was detected at WWTP- 6 may be explained as the pharmaceutical companies located around in WWTP-6.

3.3. Characterization results

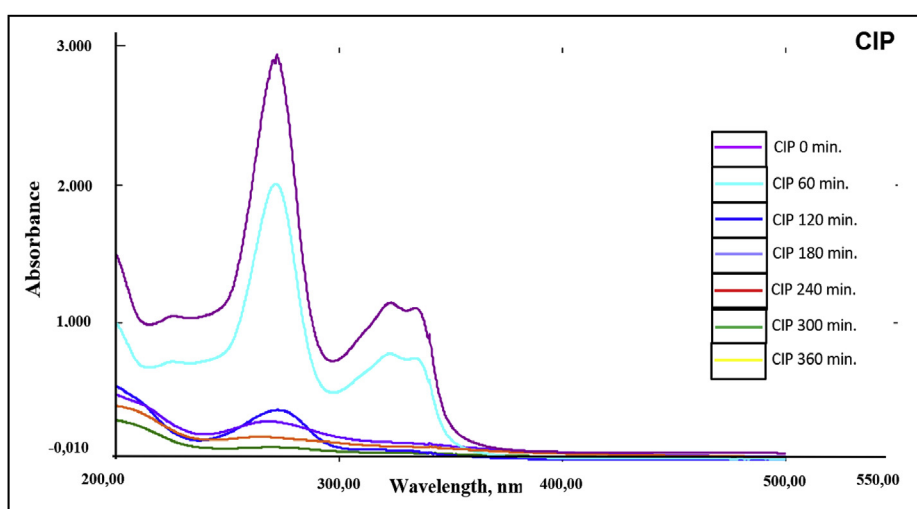
3.3.1. Characterization results of powder form of NFC-TiO₂ photocatalyst

3.3.1.1. SEM results. Powder form of anatase phase NFC-doped TiO₂ photocatalyst, specially prepared in the laboratory, was examined in terms of the morphology and particle size by using a SEM (Scanning Electron Microscope) (1.000–20.000× magnification with a resolution of 5 μm) in order to see the effects of NFC dopants on a very fine scale. The morphology of NFC-doped TiO₂ photocatalyst, at an accelerating voltage of 10 kV, is given in Fig. 2.

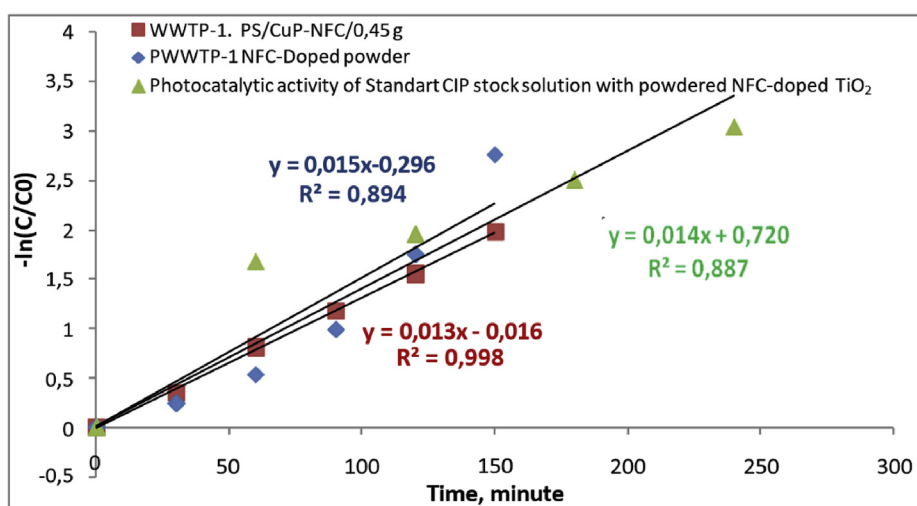
The morphology of NFC-doped TiO₂ photocatalyst was revealed by SEM analysis (Fig. 2). As seen in the figures, NFC-doped TiO₂



Graph 12. UV-Vis spectrum of CIP standard stock solution.



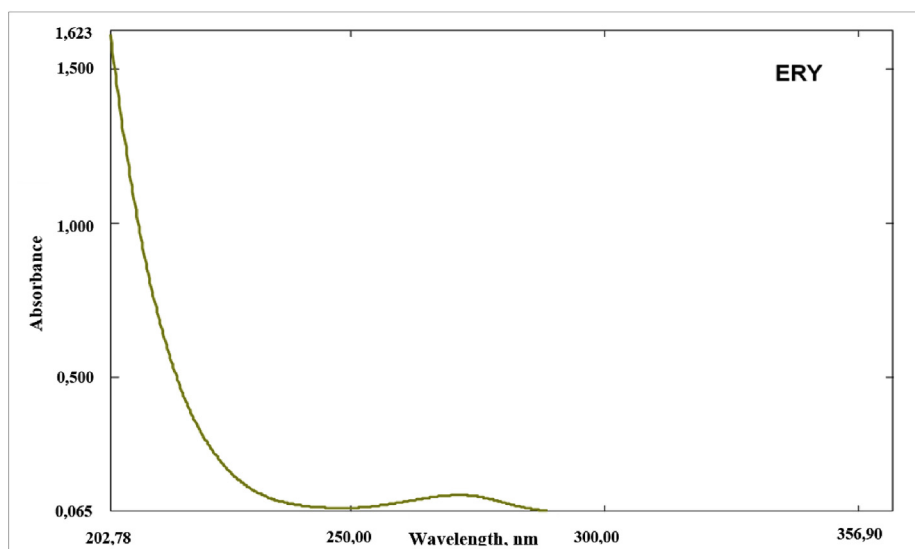
Graph 13. UV-Vis spectrum of photocatalytic activity for CIP standard stock solution with powder NFC-doped TiO₂.



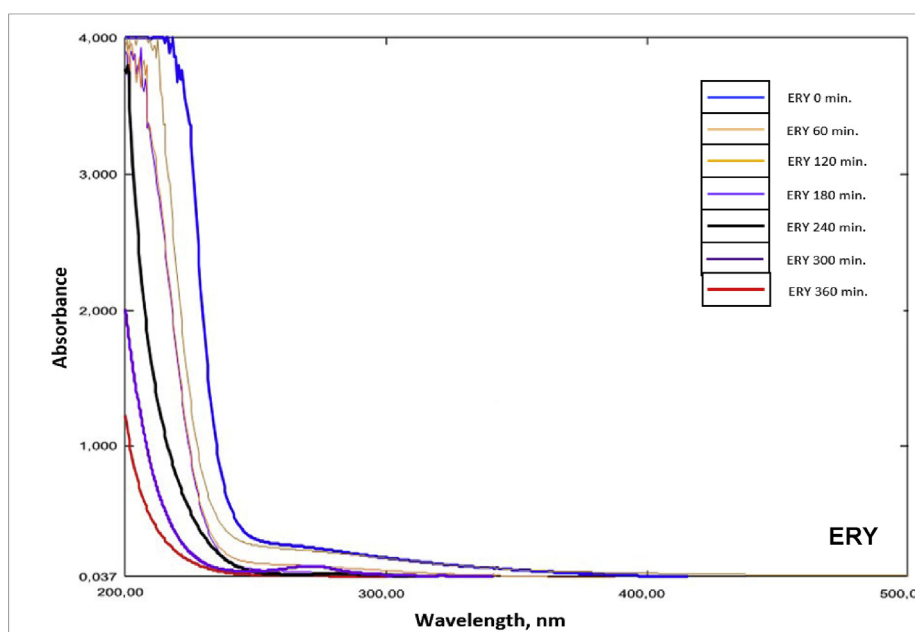
Graph 14. Comparison of the CIP standard stock solution with powder NFC-doped TiO₂ and immobilized PS/CuP-NFC 0.45 g photocatalysts in terms of kinetics of photocatalytic oxidation reactions.

photocatalyst exhibited highly porous structure which is available for photocatalyst oxidation. Aggregated particles are observable in all SEM figures and the overall network appears homogeneous.

3.3.1.2. XRD results. X-ray diffraction (XRD) measurements of the obtained yellow color anatase phase NFC-TiO₂ powder form photocatalyst, were performed with a Philips X'Pert Pro diffractometer using Cu K-



Graph 15. UV-Vis spectrum of ERY standard stock solution.



Graph 16. UV-Vis spectrum of photocatalytic activity for ERY standard stock solution with powder NFC-doped TiO₂.

alpha radiation. XRD analysis is one of the significant techniques for determining crystal structures and microstructures of chemical compositions of materials, based on diffraction experiments of atoms in materials where the diffraction pattern is observed as spectrum in it. The diffraction pattern hosts information inside for determining the crystal structures of materials with sharp and significant peaks. The angle of appearance of the two parallel rays is θ counting to Bragg's law. XRD analysis were used for the determination of the crystal phases of NFC-doped TiO₂ photocatalysts. From the results of XRD analysis and the corresponding characteristics 2θ value about 5° start position to 79° end position and 240 nm Goniometer Radius of NFC-doped TiO₂ samples (shown in Graph 4) revealed an anatase form-TiO₂ peaks observed at 25° laboratory scale conditions for all NFC-doped TiO₂ photocatalysts.

According to the XRD results, an anatase-TiO₂ peak is observed at about 25.4° for all NFC-doped TiO₂ photocatalysts indicating that it was mainly in anatase phase form. Crystallographic structure of NFC-doped TiO₂ became tetragonal after doping of TiO₂. Calculated density is

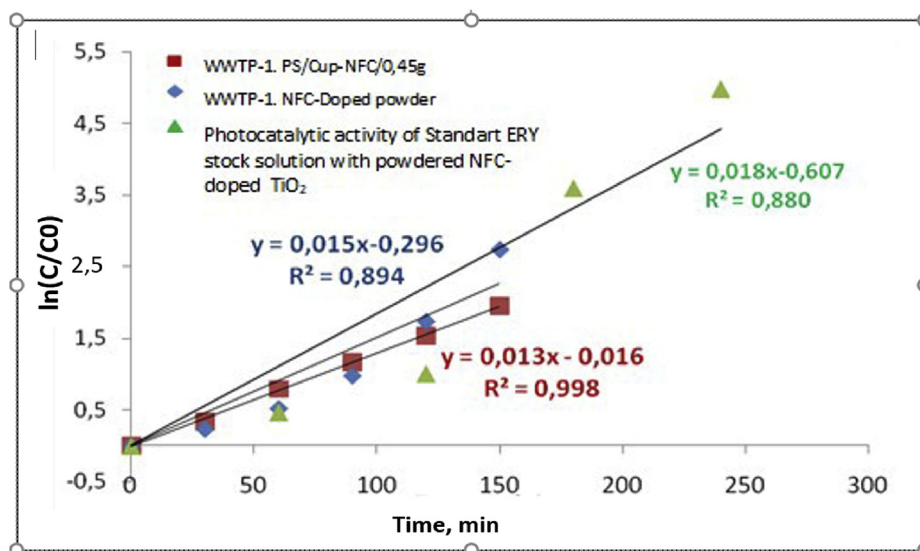
3.89 g/cm^3 and volume of cell is $136.24.106 \text{ pm}^3$.

3.3.1.3. Raman spectrum results. In addition to the XRD results, the Raman Spectrum measurements revealed that the prepared triple NFC-doped TiO₂ was a photocatalyst in an anatase form. Due to the emergence of different levels of vibration energy after the molecules interact with the photon, Raman scattering is an important element in the recognition of substances at certain wavelengths. Table 3 shows the wavelengths of typical Raman Scattering of TiO₂ [39]. Raman shift results are presented in detail in Graph 5.

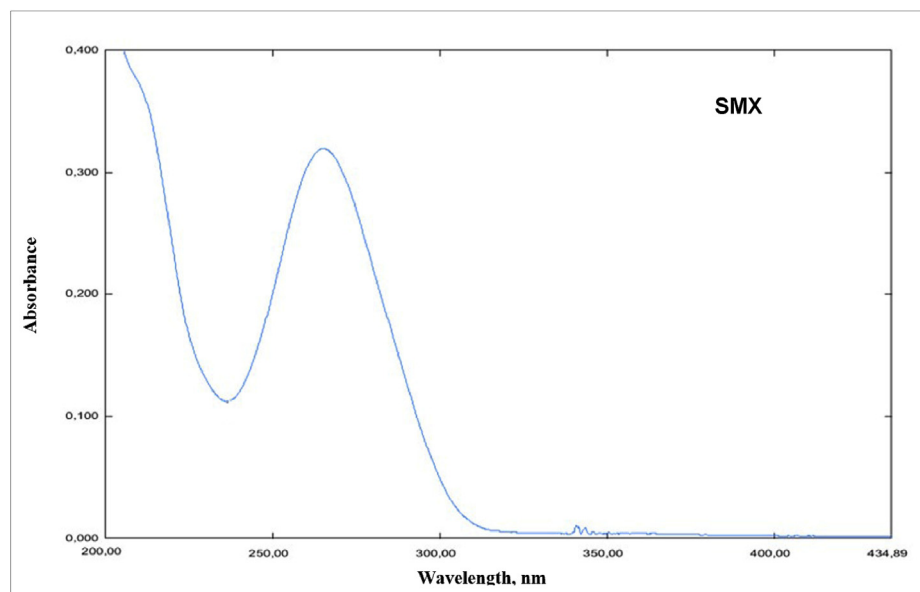
Raman shifts and wavelengths in $147, 197, 398, 516,$ and 637 cm^{-1} which were given in Graph 5 are similar to the typical Raman Shifts given in Table 3 [39]. Also, this indicates that NFC-doped TiO₂ photocatalyst is in anatase form.

3.3.2. Characterization results of immobilized PS/cup-NFC-doped TiO₂

The band gap energies of the containers prepared with immobilized



Graph 17. Comparison of the ERY standard stock solution with powder NFC-doped TiO_2 and immobilized PS/Cup-NFC/0.45 g photocatalysts in terms of kinetics of photocatalytic oxidation reactions.



Graph 18. UV-Vis spectrum of SMX standard stock solution.

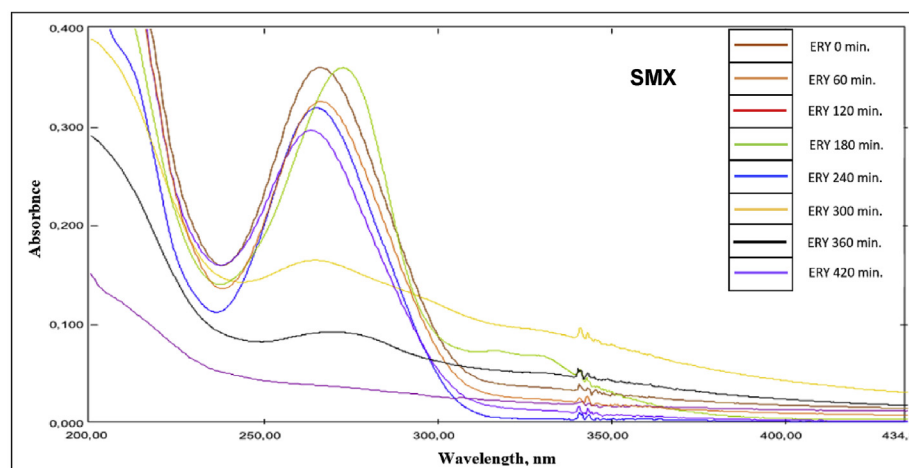
PS/Cup-NFC photocatalyst to be used in antibiotic removal (0.3 g and 0.45 g NFC doped TiO_2) were verified by Raman Shift and SEM measurements and the results were confirmed by Graph 6, Graph 7 and Fig. 3. According to the Raman shift results (Graph 7); The wavelengths of typical Raman Scattering at 143, 192, 401, 528 and 642 cm^{-1} , proving that TiO_2 is in fully anatase phase, were shown in Table 3 [39]. Graph 6 reveals that the empty container not coated with NFC-doped TiO_2 does not show raman shifts. Moreover; as it is seen from the SEM analysis results (Fig. 3.), the morphology of immobilized NFC-Doped photocatalyst was exhibited highly porous structure.

Overall network is observable in fibrillar structure providing comfortable advanced oxidation process in order to treatment of waste water. In the high magnification SEM image, an increased roughness is observed on the surface which is indicating the deposition, and isles of three different molecular structured of nanoparticles manifesting NFC-Doped TiO_2 photocatalyst.

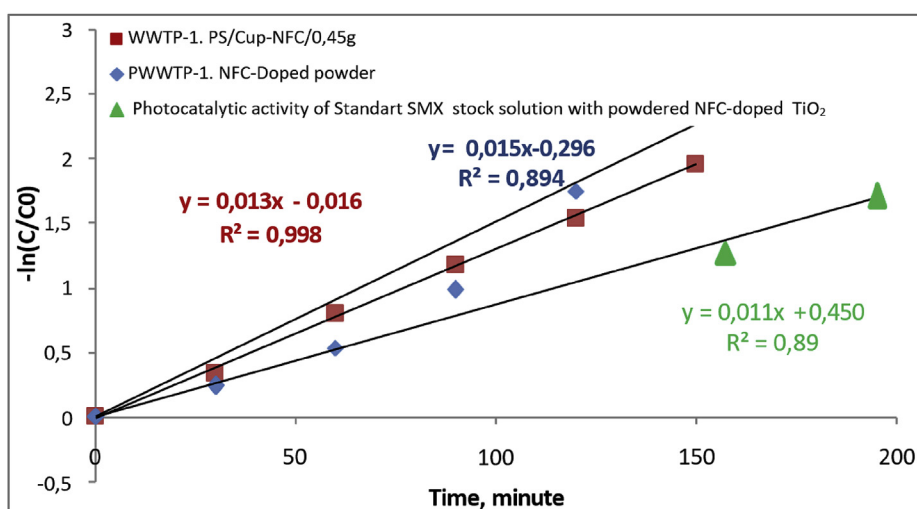
3.4. Photocatalytic oxidation study results

Efficiency results for the removal of antibiotic residues during and after photocatalytic oxidation experimental studies were evaluated in the steps outlined below;

- > Monitoring by means of measuring samples, taken hourly during photocatalytic oxidation process reactor, first in the dark and then under UV visible light by UV-Vis spectrophotometer, and evaluating the process,
- > Measuring the residual antibiotic residues, treated by photocatalytic oxidation process, by HPLC/MS-MS in order to verify the UV-Visible Spectrophotometer results,
- > After photocatalytic oxidation process, measurement of COD and TOC parameters and calculation of treatment efficiency,
- > Stabilization tests,



Graph 19. UV-Vis spectrum of photocatalytic activity of SMX standard stock solution by powder form NFC-doped TiO₂.



Graph 20. Comparison of the SMX standard stock solution with powder NFC-doped TiO₂ and immobilized PS/Cup-NFC/0.45 g photocatalysts in terms of kinetics of photocatalytic oxidation reactions.

> Evaluation of reaction kinetics.

Antibiotic removal efficiency of the urban wastewater samples taken from WWTP-1, WWTP-2, WWTP-3, WWTP-5 and industrial wastewater samples taken from WWTP-6 OSB Industrial WWTPs are given in Table 4 and Table 5.

UV-Vis Spectrophotometer measurement results and antibiotic removal efficiencies of the treated wastewater samples (WWTP-1, WWTP-2, WWTP-3, WWTP-5) effluents for urban samples and WWTP-6 Org.Ind.Distr. Effluent for industrial samples, taken hourly during the photocatalytic oxidation process, are given in Graph 8, Graph 9 and Table 6. As seen in Graph 10, when the amount of immobilized photocatalysts increased from 0.3 g to 0.45 g, it was observed that efficiency of the photocatalytic activity increasing under visible light for 420 min. Additionally, results of COD, TOC and Color treatment efficiency were given in Table 7.

As a result; in photocatalytic oxidation studies carried out with immobilized PS/Cup-NFC (0,30 g and 0,45 g) photocatalysts, the antibiotic removal efficiencies were found to be compatible with the % TOC and % COD removal results.

Furthermore, comparison of photocatalytic activities of immobilized PS/Cup-NFC/0.3 g and PS/Cup-NFC/0.45 g photocatalysts in investigated urban wastewaters is given in Graph 10.

In addition to antibiotic removal, the effect of photocatalytic activity of immobilized PS/Cup-NFC/0.45 g photocatalyst on color removal efficiency for urban and industrial wastewater was also evaluated. Color removal results are presented visually in Figs. 1 and 4 in detail in Table 8.

When the results in Table 8 are analyzed, it was revealed that WWTP-6 Industrial WWTP biologically treated effluent water, which is in the 4th grade water quality, can be upgraded to first class quality water after Advanced Photocatalytic Oxidation Process (AOP) performed with immobilized Cup-NFC/0.45 g photocatalyst.

The decrease in dissolved oxygen, conductivity and salinity parameters after photocatalytic oxidation with immobilized PS/Cup-NFC/0,45 g photocatalyst were also evaluated and the results are given in Table 9.

As seen in Table 9, treated wastewater qualities have been upgraded to mostly First Class and Second Class for both urban wastewater samples and industrial wastewater samples in terms of dissolved oxygen, conductivity and salinity parameters after photocatalytic oxidation process performed with PS/Cup-N/0,45 g. Therefore, these values show that all advanced treated wastewaters can be used in irrigational activity.

3.5. Stability and reuseability of PS/cup-NFC-doped TiO₂

For the determination of the stability of photocatalytic activity, the reuseability of the immobilized PS/Cup-NFC/0.45 g photocatalyst, with

has the highest purification efficiency, was examined by repeating photocatalytic test for 4 times. As a result of the stability test, as seen in [Graph 11](#), there was no significant decrease in the removal efficiency of organic pollutants including antibiotics. This result confirms the stability of the immobilized PS/Cup-NFC/0.45 g photocatalyst and shows that it can be reuse at least 4 times in the treatment applications.

3.6. Reaction kinetics of PS/cup-NFC-doped TiO₂

Reaction kinetics were examined to understand the mechanism of photocatalytic activities of all immobilized PS/Cup photocatalysts used in antibiotic removal from urban and industrial wastewater. Standard stock solutions for antibiotics were prepared as 1000 mg L⁻¹ in high purity water that can be used in analytical studies. After that, these standard stock solutions were diluted to different concentrations 4–250 µg mL⁻¹ and absorbances were measured in Shimadzu UV-Vis Spectrophotometer using 10 mm quartz cuvette and in pure water as blank solution.

3.6.1. Reaction mechanism and kinetics for CIP

The UV-Vis Spectrum of the CIP standard stock solution is given in [Graphic 12](#). As seen in [Graphic 12](#), the CIP showed significant peaks at 6 points. The most prominent of these peaks is at 275 nm. It was determined that the wavelength at which the first drop of the peak observed during degradation, was at 275 nm. In addition to these studies, a calibration curve was created for CIP concentrations in the range of 4–32 µg mL⁻¹ from the stock solution, thus revealing the relationship between antibiotic concentration and UV-Vis absorbance value. The R² (correlation coefficient) value of the calibration curve of CIP solutions for known concentrations was calculated as 0.999 (very close to 1) and it was found to have a 1st order reaction kinetics. This result showed a linear relationship between the concentration of CIP standard solution and its absorbivity.

After that, photocatalytic oxidation experiments were carried out to remove the CIP antibiotic in the 4 µg mL⁻¹ aqueous CIP standard stock solution by means of NFC-doped TiO₂. In these experimental studies, photocatalytic activity of powder NFC-doped TiO₂ with the highest rate of removal of the CIP, is given in [Graph 13](#). Besides, when the kinetics of the CIP removal photocatalytic activity reaction, with powder form NFC-doped TiO₂, were examined, it was found that the CIP standard stock solution could be expressed by a first order reaction kinetics of 0.899 R². Moreover, comparing the kinetics of the photocatalytic oxidation reactions of CIP antibiotics in WWTP-1 Urban Effluent (containing higher amount of CIP residues compared to other urban wastewater samples) with PS/Cups-NFC-doped TiO₂ photocatalysts powder form NFC-doped TiO₂ and standard CIP solution examined, the reaction rate constants were found very close to each other and determined as 0.013, 0.015 and 0.014, respectively ([Graph 14](#)).

In addition, the very high correlation value of R in all three-reaction kinetics showed that there is a strong correlation between the CIP removal detected by UV-Vis Spectrophotometer measurements and by HPLC-MS/MS results. This reveals that the photocatalytic activity is not affected by diffusion [40] and only the NFC-TiO₂ photocatalyst, coated on the PS inner surface, played an active role in the reaction therefore, advanced oxidation occurred directly. In all three-reaction kinetics, it was observed that the target pollutant removal reaction after dark adsorption conformed to the first order kinetic formula.

3.6.2. Reaction mechanism and kinetics for ERY

The UV-Vis Spectrum of the ERY standard stock solution is given in [Graph 15](#). As seen in the graph, ERY showed distinct peaks at 2 wavelengths. The most prominent of these peaks were around 250 nm and other smaller one around 285 nm. In addition, a calibration curve was created for CIP concentrations in the range of 35–181 µg mL⁻¹ from the stock solution, thus revealing the relationship between antibiotic concentration and UV-Vis absorbance value.

The R² (correlation coefficient) value of the calibration curve for ERY solutions in known concentrations, was calculated as 0.9946 (very close to 1) and found to have a 1st degree reaction kinetics. It revealed a linear relationship between the concentration of ERY standard solution and its absorbivity of UV-visible light. After that, photocatalytic oxidation experiments were carried out to remove ERY from the 4 µg mL⁻¹ ERY standard stock solution by using powder form NFC-doped TiO₂ photocatalyst. Photocatalytic activity of powder form NFC-doped TiO₂ for removal of ERY, is given in [Graph 16](#).

In [Graph 17](#), constants of the reaction kinetics were calculated for photocatalytic oxidation performed with WWTP-1 Urban effluent waste water containing high amounts of ERY residues. ERY standard stock solution were found very close to PS/Cup-NFC 0.45 g photocatalysts and powder form of NFC-doped TiO₂ as 0.013, 0.015 and 0.018, respectively.

Therefore, R correlation value, which was very high as reaction kinetics, showed that both there is a strong correlation between the ERY removal detected by UV-Vis Spectrophotometer measurements and the exact results performed by HPLC-MS/MS and also photocatalytic activity was not affected by diffusion spreads [40]. In the reaction under the photochemical condition, NFC-TiO₂ photocatalyst, coated only onto the inner surface of the PS, played an active role and thus directly photochemical oxidation occurred. Furthermore, in all three-reaction kinetics, it was observed that the target pollutant removal reaction after dark adsorption conformed to the first order kinetic formula.

3.6.3. Reaction mechanism and kinetics for SMX

The UV-Vis Spectrum of SMX standard stock solution, which was harder to degrade than other antibiotics, is given in [Graph 18](#). As seen in the [Graph 18](#), SMX showed peaks around at 240 nm and at 265 nm. By the way, a calibration curve for SMX concentrations in the range of 64–251 µg mL⁻¹ was created from the stock solution, revealing the relationship between antibiotic concentration and UV-Vis absorbance value.

The R² (correlation coefficient) value of the calibration curve of SMX solutions in known concentrations was calculated as 0.998 (very close to 1) and found to have a 1st degree reaction kinetics. It is determined that a linear relationship between the concentration of SMX standard solution and its absorbivity of UV-visible light. Photocatalytic oxidation experiments were carried out to remove the SMX in 4 µg mL⁻¹ aqueous SMX standard stock solution by powder form of NFC-doped TiO₂ photocatalyst. Photocatalytic activity of powder form of NFC-doped TiO₂, with the highest rate of removal of the SMX antibiotic, is given in [Graph 19](#).

The reaction kinetics of photocatalytic oxidation, performed with WWTP-1 Urban effluent, containing high amounts of SMX residues and SMX standard stock solution were determined as 0.013, 0.015 and 0.011, respectively ([Graph 20](#)). Therefore, the fact that R correlation value was very high in reaction kinetics proving both there is a strong correlation between ERY removal detected by UV-Vis Spectrophotometer measurements and the results performed by HPLC-MS/MS and photocatalytic activity was not affected by diffusion spreads. It means NFC-TiO₂ photocatalyst, coated only on to the inner surface of the PS, played an active role and provided directly photocatalytic oxidation.

Furthermore, it was determined that the target pollutant removal reaction, after dark adsorption, complied with the first degree kinetics in all three reaction kinetics.

When the results of the kinetic reaction analysis were evaluated for all 3 antibiotics, it was determined that HPLC/MS-MS measurements gave definite results in the removal of antibiotic residues within the scope of this study. Therefore, UV-Vis Spectrophotometer measurements can be recommended as an alternative method to monitor the progress of the process during photocatalytic oxidation and also to monitor the removal of color and organic contaminants containing antibiotic residues.

4. CONCLUSION

In this study, it was determined that urban wastewater, examined in

terms of conventional pollutants, has medium level and industrial wastewater has high organic load in terms of TOC and COD. Considering the characterization results of the analyzed waste water in terms of antibiotic residues, despite the biological treatment process, it was determined that the effluent in the WWTPs has been found to contain higher amounts of antibiotic residues than the untreated raw influents. This indicates that antibiotic removal cannot be achieved with conventional systems and supports the comments in the literature that metabolite formation during biological oxidation causes an increase in antibiotic residues in wastewater. As a result of the photocatalytic oxidation studies, performed using the PS/Cup-NFC photocatalyst immobilized with powdered NFC-doped TiO₂ photocatalyst, the removal efficiency of antibiotic residues and color contaminants was evaluated with HPLC/MS-MS, UV-Vis Spectrophotometer, COD and TOC measurement results. Removal ratios for antibiotics and organic substances with immobilized P/Cup-NFC photocatalyst were found as 97%~100% for CIP, 100% for ERY and 86%~100% for SMX, 57%~64% for COD and 61,5~72% for TOC.

Moreover, in terms of immobilized photocatalysts in PS/Cup form, it was observed that as the amount of powder photocatalyst plastered onto the inner surface of PS was increased, antibiotic residue removal performance was also increased and its optimum value was determined as 0.45 g. On the other hand in terms of removal of color pollution, it has been determined that a 4th class water quality industrial treated wastewater can be upgraded to 1st class water quality by means of photocatalytic oxidation with immobilized PS/Cup-NFC.

In addition, when the antibiotic residue removal efficiencies between powdered and immobilized photocatalysts were evaluated, it was determined that the photocatalytic activities of powder photocatalysts under visible light were almost at the same level with immobilized photocatalysts. However, considering the advantages of immobilized photocatalysts such as not leaving chemical waste and reusing in purified water after photocatalytic oxidation process, it can be recommended as an alternative to powder photocatalysts. Far better, for the first time, with this study, it was revealed that UV-Vis Spectrophotometer measurement results, which were found to be compatible with HPLC measurements, can be used as an effective method in experimental studies to remove antibiotic residues by photocatalytic oxidation.

Finally, according to the results of this study, it was determined that photocatalytic oxidation processes can be performed under visible light with specially prepared powder (NFC doped TiO₂) and immobilized form (PS/Cup-NFC/0.45 g) photocatalysts in the laboratory conditions with a cheap and economic method. This can be an alternative advanced treatment method to remove antibiotic residues and color residues from Urban and Industrial wastewater which cannot be treated effectively by conventional WWTPs.

Declaration of competing interest

The author(s) declare(s) that there is no conflict of interest.

Acknowledgement

This study was supported by the Scientific Research Council of Tekirdağ Namık Kemal University via Grant No. NKUBAP.06.GA.16.053.

Appendix A. Supplementary data

Supplementary data to this article can be found online at <https://doi.org/10.1016/j.crgsc.2021.100065>.

References

- [1] M. Hansen, K.A. Krogh, A. Brandt, J.H. Christensen, B. Halling-Sørensen, Fate and antibacterial potency of anticoccidial drugs and their main abiotic degradation products, *Environ. Pollut.* 157 (2009) 474–480.
- [2] C. Xi, Y. Zhang, C.F. Marrs, W. Ye, C. Simon, B. Foxman, Prevalence of antibiotic resistance in drinking water treatment and distribution system, *Appl. Environ. Microbiol.* 75 (2009) 5714–5722.
- [3] H. Storteboom, M. Arabi, J.G. Davis, B. Crimi, A. Pruden, Tracking antibiotic resistance genes in the south Platte river basin using molecular signatures of urban, agricultural, and pristine sources, *Environ. Sci. Technol.* 44 (2010) 7397–7404.
- [4] M. Munir, K. Wong, I. Xagorarakis, Release of antibiotic resistant bacteria and genes in the effluent and biosolids of five wastewater utilities in Michigan, *Water Res.* 45 (2011) 681–693.
- [5] N. Le-Minh, R.M. Stuetz, S.J. Khan, Determination of six sulfonamide antibiotics, two metabolites and trimethoprim in wastewater by isotope dilution liquid chromatography/tandem mass spectrometry, *Talanta* 89 (2012) 407–416.
- [6] P. Gao, M. Munir, I. Xagorarakis, Correlation of tetracycline and sulfonamide antibiotics with corresponding resistance genes and resistant bacteria in a conventional municipal wastewater treatment plant, *Sci. Total Environ.* 421–422 (2012) 173–183.
- [7] K.A. Rickman, S.P. Mezyk, Kinetics and mechanisms of sulfate radical oxidation of β -lactam antibiotics in water, *Chemosphere* 81 (2010) 359–365.
- [8] C.-W. Yang, C. Liu, B.-V. Chang, Biodegradation of amoxicillin, tetracyclines and sulfonamides in wastewater sludge, *Water* 12 (2020) 2147, <https://doi.org/10.3390/w12082147>.
- [9] L.B. Barber, S.H. Keefe, D.R. LeBlanc, P.M. Bradley, F.H. Chapelle, M.T. Meyer, K.A. Loftin, D.W. Kolpin, F. Rubio, Fate of sulfamethoxazole, 4-nonylphenol, and 17 β -estradiol in groundwater contaminated by wastewater treatment plant effluent, *Environ. Sci. Technol.* 43 (2009) 4843–4850.
- [10] M. Qiao, G.G. Ying, A.C. Singer, Y.G. Zhu, Review of antibiotic resistance in China and its environment, *Environ. Int.* 110 (2018) 160–172.
- [11] K.E. Gzyl, H.J. Wieden, Tetracycline does not directly inhibit the function of bacterial elongation factor Tu, *PLoS One* 12 (2017), e0178523.
- [12] K.S. Yalap, I.A. Balcioglu, Effect of water components on the treatment of oxytetracycline with advanced oxidation, *ITU J. Water Pollut. Contr. Issue* 18 (2–3) (2008) 51–60.
- [13] L. Delibas, Optimum Planning and Management in Large Irrigation Networks. IV. National Agricultural Structures and Irrigation Congress Proceedings, Atatürk University Faculty of Agriculture, Department of Farm Structures and Irrigation, Erzurum, Turkey, 2010, pp. 25–35.
- [14] R. Thiruvenkatachari, S. Vigneswaran, II S. Moon, A review on UV/TiO₂ photocatalytic oxidation process, *Kor J. Chem. Eng.* 25 (1) (2008) 64–72, <https://doi.org/10.1007/s11814-008-0011-8> (Journal Review).
- [15] P. Wang, P.S. Yap, T.T. Lim, C–N–S tridoped TiO₂ for photocatalytic degradation of tetracycline under visible-light irradiation, *Appl. Catal.* 399 (2011) 252–261.
- [16] R. Ata, G. Yıldız Töre, Characterization and removal of antibiotic residues by NFC-doped photocatalytic oxidation from domestic and industrial secondary treated wastewaters in Meric-Ergene Basin and reuse assessment for irrigation, *J. Environ. Manag.* 233 (2019) 673–680, <https://doi.org/10.1016/j.jenvman.2018.11.095>.
- [17] Y. Xu, Y. Zhuang, X. Fu, New insight for enhanced photocatalytic activity of TiO₂ by doping carbon nanotubes: a case study on degradation of benzene and methyl orange, *J. Phys. Chem. C* 114 (2010) 2669.
- [18] H. Liu, W. Zhang, ZnO nanoparticles anchored on nickel foam with graphene as morphology-controlling agent for high-performance lithium-ion battery anodes, *J. ACS Appl. Mater. Interfaces* 3 (2011) 1757.
- [19] D. Christian, A.P.-O. Miguel, S.K. Christopher, Punke Paul, E.P. Christopher, J. Peter, G. Feliciano, J.J. Soon, K. Kalus, TiO₂ Anatase with a Bandgap in the Visible Region, *American Chemical Soc.* 2014, <https://doi.org/10.1021/nl50313s>.
- [20] R. Asahi, T. Morikawa, T. Ohwaki, K. Aoki, Y. Taga, Visible-light photocatalysis in nitrogen doped titanium oxides, *Science* 293 (2001) 269–271.
- [21] S.M. El-Sheikh, G. Zhang, H.M. El-Hosainy, A.A. Ismail, K.E. O'Shea, P. Falaras, A.G. Kontos, D.D. Dionysiou, High performance sulfur, nitrogen and carbon doped mesoporous anatase-brookite TiO₂ photocatalyst for the removal of microcystin-LR under visible light irradiation, *J. Hazard Mater.* 280 (2014) 723–733.
- [22] O. Sacco, M. Stoller, V. Vaiano, P. Ciambelli, A. Chianese, D. Sannino, Photocatalytic degradation of organic dyes under visible light on N-doped TiO₂ photocatalysts, *Int. J. Photoenergy* (2012), <https://doi.org/10.1155/2012/626759>. Article ID 626759, 8 pages.
- [23] L.G. Devi, R. Kavitha, A review on non metal ion doped titania for the photocatalytic degradation of organic pollutants under UV/solar light: role of photogenerated charge carrier dynamics in enhancing the activity, *Appl. Catal. B Environ.* 140–141 (2013) 559–587.
- [24] D. Li, H. Haneda, S. Hishita, Ohashi, N. Chem. Mater. 17 (2005) 2588.
- [25] D. Li, H. Haneda, S. Hishita, Ohashi, N. Chem. Mater. 17 (2005) 2596.
- [26] N. Miranda-García, M.I. Maldonado, J.M. Coronado, S. Malato, Degradation study of 15 emerging contaminants at low concentration by immobilized TiO₂ in a pilot plant, *Catal. Today* 151 (1) (2010) 107–113, <https://doi.org/10.1016/j.cattod.2010.02.044>.
- [27] Y. Wang, Y. Huang, W. Ho, L. Zhang, Z. Zou, S. Lee, Biomolecule-controlled hydrothermal synthesis of C–N–S-tridoped TiO₂ nanocrystalline photocatalysts for NO removal under simulated solar light irradiation, *J. Hazard Mater.* 169 (2009) 77–87.
- [28] G. Zhang, Y. Zhang, M. Nadagouda, C. Han, K. O'Shea, S.M. El-Sheikh, A.A. Ismail, D.D. Dionysiou, Visible light-sensitized S, N and C co-doped polymorphic TiO₂ for photocatalytic destruction of microcystin-LR, *Appl. Catal., B* 144 (2014) 614–621.
- [29] X. Cheng, X. Yu, Z. Xing, One-step synthesis of visible active C–N–S-tridoped TiO₂ photocatalyst from biomolecule cystine, *Appl. Surf. Sci.* 258 (2012) 7644–7650.
- [30] X. Cheng, X. Yu, Z. Xing, Synthesis and characterization of C–N–S-tridoped TiO₂ nano-crystalline photocatalyst and its photocatalytic activity for degradation of rhodamine B, *J. Phys. Chem. Solid.* 74 (2013) 684–690.

- [31] X. Lin, D. Fu, L. Hao, Z. Ding, Synthesis and enhanced visible-light responsive of C,N,S-tri doped TiO₂ hollow spheres, *J. Environ. Sci.* 25 (2013) 2150–2156.
- [32] ISO 6060, Water Quality - Determination of the Chemical Oxygen Demand, 1986. Reference No: 6060–1986.
- [33] ISO 7887, Water Quality - Examination and Determination of Colour, 2011.
- [34] APHA, Standard Methods for the Examination of Water and Wastewater, 1998, twentieth ed., American Public Health Association/American Water Works Association/Water Environment Federation, Washington DC, USA, 1998.
- [35] R. Ata, O. Sacco, V. Vaiano, L. Rizzo, G. Yıldız Töre, D. Sannino, Visible light active N- doped TiO₂ immobilized on polystyrene as efficient system for wastewater treatment, *J. Photochem. Photobiol. Chem.* 348 (2017) 255–262.
- [36] Surface Water Quality Regulation, Quality Parameters in Terms General Chemical and Physicochemical of Intracratonic Surface Water Sources, 2004. Annex 5, Table 2.
- [37] J.C. Chee-Sanford, R.I. Mackie, S. Koike, I.G. Krapac, Y.-F. Lin, A.C. Yannarell, S. Maxwell, R.I. Aminov, May, Fate and transport of antibiotic residues and antibiotic resistance genes following land application of manure waste, *J. Environ. Qual.* 38 (3) (2009) 1086–1108, <https://doi.org/10.2134/jeq2008.0128>.
- [38] D.I. Massé, N.M.C. Saady, Y. Gilbert, Potential of biological processes to eliminate antibiotics in livestock manure: an overview, *Animals* 4 (2014) 146–163, <https://doi.org/10.3390/ani4020146>.
- [39] T. Ohsaka, F. Izumi, Y. Fujiki, Raman spectrum of anatase, TiO₂, *J. Raman Spectrosc.* 7 (6) (1978) 321–324.
- [40] V. Vaiano, O. Sacco, D. Sannino, P. Ciambelli, Nanostructured N-doped TiO₂ coated on glass spheres for the photocatalytic removal of organic dyes under UV or visible light irradiation, *Appl. Catal. B Environ.* 170–171 (2015) 153–161.